Lasers in Medical Science (2019) 34:1645–1654
https://doi.org/10.1007/s10103-019-02761-0

ORIGINAL ARTICLE

Transcutaneous transmission of photobiomodulation light to the spinal canal of dog as measured from cadaver dogs using a multi-channel intra-spinal probe

Daqing Piao[1,2] · Lara A. Sypniewski[1] · Danielle Dugat[1] · Christian Bailey[2] · Daniel J. Burba[1] · Luis DeTaboada[3]

Received: 2 October 2018 / Accepted: 26 February 2019 / Published online: 16 March 2019

Abstract

The target level photobiomodulation (PBM) irradiances along the thoracic to lumbar segment of the interior spinal canal in six cadaver dogs resulting from surface illumination at 980 nm were measured. Following a lateral hemi-laminectomy, a flexible probe fabricated on a plastic tubular substrate of 6.325 mm diameter incorporating nine miniature photodetectors was embedded in the thoracic to lumbar segment of the spinal canal. Intra-spinal irradiances at the nine photodetector sites, spanning an approximate 8 cm length caudal to T13, were measured for various applied powers of continuous wave (CW) surface illumination at 980 nm with a maximal power of 10 W corresponding to a surface irradiance of 3.14 W/cm^2. The surface illumination conditions differed in skin transmission when the probe was off-contact with tissue and probe-skin contact when the skin was in place. For each condition of surface illumination, the beam was directed to respectively T13 (surface site 1), a spinal column site 4 cm caudal to T13 (surface site 5), and a spinal column site 8 cm caudal to T13 (surface site 9). Off-contact surface irradiation of 3.14 W/cm^2 at surface sites 1, 5, and 9 transmitted respectively 234.0 ± 120.7 μW/cm^2, 230.7 ± 178.3 μW/cm^2, and 130.2 ± 169.6 μW/cm^2 to the spinal canal without the skin, and respectively 35.7 ± 33.2 μW/cm^2, 50.9 ± 75.3 μW/cm^2, and 15.7 ± 16.3 μW/cm^2 with the skin. Transmission with skin was as low as 12% of the transmission without the skin. On-contact surface irradiation of 3.14 W/cm^2 at surface sites 1, 5, and 9 transmitted respectively 44.6 ± 43.1 μW/cm^2, 85.4 ± 139.1 μW/cm^2, and 22.0 ± 23.6 μW/cm^2 to the spinal canal. On-contact application increased transmission by a maximum of 67% comparing to off-contact application. The information gathered highlights the need to clinically consider the impact of skin transmission and on-contact application technique when attempting to treat spinal cord disease with PBM.

Keywords Photobiomodulation · Low-level light therapy · 980 nm · Dosimetry · Spinal cord injury · Transcutaneous

Introduction

Traumatic spinal cord injuries, degenerative spinal cord diseases, and chronic neuropathic pain are all neurological lesions which negatively affect the function, wellness, and overall quality of life for both humans and animals. In general, the management of spinal cord disease and injury involves a combination of medical and surgical interventions with intense rehabilitation to optimize functional outcomes [1]. There are a number of ongoing trials seeking alternative treatment strategies to mitigate the effects of spinal cord injuries and disease including anesthetics, neurosurgical procedures, psychotherapy, and physiotherapeutic resources [2]. Photobiomodulation (PBM) is a non-invasive treatment application that has been investigated broadly in human and veterinary medicine and is a modality that may impact spinal cord physiology to improve patient outcomes.

The goal of spinal cord intervention is to "rescue, reactivate, and rewire" the neuronal network [3]. Tissue rescue prevents damage beyond the primary site of injury and is obtained through surgical means or via modalities that target

✉ Daqing Piao
daqing.piao@okstate.edu

[1] Department of Veterinary Clinical Sciences, Center for Veterinary Health Sciences, Oklahoma State University, Stillwater, OK 74078, USA

[2] School of Electrical and Computer Engineering, Oklahoma State University, Stillwater, OK 74078, USA

[3] LiteCure LLC, Carlsbad, CA 92008, USA

inflammation [3]. PBM has shown to reduce inflammation through a reduction in fibrinogen levels, edema, and inflammatory cell presence [4, 5]. This intervention also reduces pain by reducing inflammation; additional analgesia may also be a by-product of an increased synthesis of endorphins [6]. Tissue reactivation refers to how spared systems can be utilized to stimulate spinal networks or re-myelinate denuded axons [3]. PBM investigations in neuronal regeneration have demonstrated stimulation of axonal regrowth of the spinal cord after acute structural damage in rodent models [1, 7, 8]. Although the mechanism for axonal regeneration is unknown, it has been theorized to be secondary to inflammatory cell inhibition which alters the extra-cellular milieu providing a local environment which may encourage axonal regrowth [1]. Tissue rewiring is based on treatments focused on regrowth of damaged axons or readapting spared ones [3]. Transcranial PBM is reported to improve cerebral neurological functions by ameliorating mitochondrial dysfunction and modulating effects on apoptosis [9] as well as maintaining mitochondrial survival by improving the antioxidant defense system [10]. PBM interventions to preserve and maintain cerebral mitochondrial function and attenuate oxidative stress [10] theoretically could have similar physiologic effects on the spinal cord.

In order to treat the spinal cord and surrounding tissues, PBM treatments must penetrate deeply without causing collateral damage to the surface or target tissues. The anatomical safeguards of heavy muscle cover and tall vertebral processes make delivery of PBM to the spinal cord exceedingly challenging; significant treatment dose attenuation occurs as the PBM light passes through tissue and bone. Class IV lasers provide longer wavelengths (up to 1064 nm) with higher power outputs and activate therapeutic cellular metabolic changes in deep tissue [11] but has shown to not be effective if the terminal irradiance (or dose) is below a therapeutic threshold. Evaluation of the target tissue dose is essential in determining the therapeutic surface dose ranges.

As noted by de Andrade et al. in regard to PBM research, study comparison was problematic as many studies lacked detailed PBM irradiance or energy density parameters, thereby making it difficult to suggest efficacious treatment protocols [2]. Clinical evaluation of the action of PBM radiation requires consideration of the energy applied to surface tissue, the effective transmission of the energy density or total power specific to a wavelength, and finally the terminal dose that reaches the target tissue [2]. The literature suggests the use of PBM at infrared wavelengths (780 to 905 nm) at powers between 30 and 450 mW may be effective in treating neuropathic pain in experimental models, suggesting these PBM wavelengths are able to penetrate tissue and bone to reach the level of the spinal cord to impact neural tissue [2].

As PBM effects are dose-dependent, the applied dose must be selected to minimize collateral thermal damage but be adequate to produce the desired bio-modulatory therapeutic response. Clinical transcutaneous administration must consider the irradiance to be safe and the exposure time to be manageable. The treatment dose (energy/area) is delivered with either a stronger target-level irradiance over a shorter exposure time or a weaker target-level irradiance over a longer exposure time. In rodent models of SCI tested for PBM, a high skin-to-spine penetration of 6% was measured at 810 nm [1]. For clinical therapy in larger mammals, high skin-to-spine PBM dose transmission is not expected due to the thick and complex anatomy which may prevent transmission of therapeutic irradiance/dose to the spinal cord. In addition, the surface irradiation/dose required to overcome anatomy may result in collateral thermal damage at the surface. The complex skin-to-spine tissue anatomy as well as its associated optical properties makes it challenging to accurately estimate the skin-to-spine transmission of light of therapeutic wavelength using simulations. Consequently, inaccurate estimation of the terminal irradiance/dose to the spinal canal using a simple model of tissue transmission could result in sub-therapeutic target-level irradiation or the target-level irradiation surpassing not only the thermal threshold of surrounding anatomic structures, but also the thermally-sensitive spinal cord itself [12]. Mitigating collateral thermal damage is essential in clinical applications and must be considered in evaluating treatment dosages. Currently, the threshold of PBM dose or irradiance at 660–670 nm [13, 14], 780 nm [15, 16], and 808–810 nm [1, 7, 8, 17–20] for treating spinal cord disease based on experimental data from rodents has not been well established.

The effectiveness of PBM for rodent models of spinal cord injury (SCI) was demonstrated at a terminal irradiance of ~ 3.2 mW/cm^2 [14]. This target dose corresponds with a transcutaneous transmission of 10^{-3} for a surface irradiance of 3.2 W/cm^2. This surface power is challenging but not impractical as it can be administered with 10 W of uniform power over a beam area slightly less than 2 cm in diameter. A 10^{-3} transmission, however, could be a significant overestimation of light penetration that can be achieved at the spinal cord level. It is currently unknown if a therapeutic target-level irradiance of 3.2 mW/cm^2 can be delivered transcutaneously to reach the level of the spinal cord with a clinically manageable surface irradiation protocol. Experimental measurements are thus needed to estimate the clinical transcutaneous transmission of light to the spinal cord at wavelengths with therapeutic potential.

A 980-nm 10-W fiber-coupled laser source and a flexible nine-channel photodetector probe having a spectral response over 750–1100 nm [21] have been accessed for multi-site irradiance measurements at the level of the spinal cord. The flexible probe of 8 cm in length composing nine mini-photodetectors can be embedded in the spinal canal of a dog cadaver through an incision for intra-spinal dosimetry. With access to the probe, our team's objectives were to report the

target level irradiance at the level of the spinal canal using transcutaneous transmission of CW 980 nm light in six large breed cadaver dogs and evaluate surface application technique's effect on target-level dosimetry. This dosimetry information will guide clinical applications by determining the transcutaneous transmission of PBM light and its subsequent attenuation, providing information on the actual dose that reaches the spinal canal target.

Methods and materials

The flexible multi-channel dosimetry probe and the interfacing device

The probe fabrication, device configuration, and irradiance calibration of the flexible nine-channel probe were detailed in [21]. Briefly, the probe integrated nine surface mounting silicon PIN type photodiodes (PDs) with a spectral response over 750–1100 nm (SFH2400FA-Z, OSRAM Opto Semiconductors GmbH, Regensburg, Germany) at 10 mm intervals onto a flexible tubular substrate of 6.325 mm in diameter. Each PD sensor was conditioned individually to convert the photocurrent to a voltage signal. Eight of the nine PD sensor read-out channels were computer interfaced for concurrent monitoring and logging via a graphical user interface (GUI). The ninth PD read-out channel was manually registered via a precision multi-meter. Irradiance calibration was performed at 850 nm, at which the photodiode's responsivity is approximately the same as that at 980 nm. The photoresponsivity of all nine PDs were set at producing 1 V per 7.58 $\mu W/cm^2$ continuous-wave (CW) irradiance at 850 nm or 980 nm, configured by using a sensing resistor of 22 MΩ.

Measurement protocol for intra-spinal dosimetry with cadaver dogs

Cadaver dogs were used to accommodate the size of the flexible probe for intra-spinal deployment and to inform transmission at a skin-to-spine scale that parallels companion care and clinical translation. The use of cadaver dogs for this study was exempted by the Institutional Animal Care and Use Committee of the University. Six cadaver dogs (male, mixed breed) weighing 18.9 to 37.2 kg were obtained from a regional animal shelter. The dogs were euthanized because of terminal conditions not affecting the dermis, musculature, bones, and nervous system. The six dogs were acquired two at a time over three randomly selected dates of 3 to 4 weeks apart. The cadavers were delivered frozen, and thawed and used within 48 h. The dorsum of the cadaver dog was clipped (Oster A5 Cordless Clipper/#40 clipper blade/Valley Vet Supply, Marysville, KS, USA) caudal to the spinous process of T9 to the lumbo-sacral junction to allow for surgical access. Following a lateral hemi-laminectomy, the spinal cord was removed in order to expose the spinal canal extending from approximately T12 to L6 vertebral sections. The flexible nine-channel photodetector probe with a substrate stem of 6.325 mm in diameter was embedded within the exposed spinal canal with the wiring sorted for channels 1 to 9 directed caudally to the interfacing device. The most cranially placed sensor, PD 1 of the probe, was aligned to T13 with the position marked on the tissue surface using a 22-gauge hypodermic needle. The nine PD sensors embedded in epoxy pockets in direct contact with the dorsal wall of the spinal canal lumen faced the treatment beam through the vertebra. After the probe placement within the spinal canal, peripheral muscle and fascia tissues were opposed and closed at each level with full thickness simple interrupted sutures (3-0 PDS, Ethicon) to provide a continuous tissue environment. The tissues were moistened to ensure an appropriate seal and water was instilled in the area to help remove air between tissue layers and within the spinal canal.

The 980 nm beam emitted from a conic treatment head connected to a companion laser unit (Model CTS, LiteCure LLC, Newark, DE) was positioned by using a heavy-duty articulated arm at three probe-tissue configuration: (1) off-contact without the skin or 1 cm from the tissue not covered by skin, (2) off-contact with the skin or 1 cm from the tissue covered by skin, and (3) on-contact with the skin. For each probe-tissue configuration the beam was directed to three positions along the spinal column, including T13 (referred to as surface site 1), a spinal column site 4 cm caudal to T13 (referred to as surface site 5), and a spinal column site 8 cm caudal to T13 (referred to as surface site 9), which corresponded to respectively the channel 1 (cranial aspect), channel 5 (middle aspect), and channel 9 (caudal aspect) of the intra-spinal probe containing nine PDs over an 8-cm spinal column length.

Statistical analysis

The main objective of the study was to measure the irradiance of 980 nm light at the spinal cord level under a surface irradiance up to 3.14 W/cm^2. The measurements that differed only in whether the skin was absent or present in the beam path were used to evaluate skin attenuation to the transmission. Similarly, the measurements that differed only in whether the probe was off-contact or on-contact with tissue were used to assess the effect of probe-tissue contact on transmission. These data groups for evaluating skin attenuation or contact effect had the same data structures and sample sizes; therefore, those data groups were subjected to paired t tests using GraphPad Prism 6 [GraphPad Software, La Jolla, CA]. A p value of < 0.05 was considered to infer statistically significant

differences. The results are presented as mean value and the standard deviation (SD).

Results

Intra-spinal irradiance under a surface irradiation at various spinal locations—a representative set

A total of 3492 intra-spinal irradiances were acquired. Figure 1 presents the representative intra-spinal irradiances over an 8-cm length of the spinal canal of dog 5 (34.35 kg) as measured by the nine-channel photodetector probe that differed in skin transmission. The upper panel of each column corresponds to off-contact of the beam to the tissue without skin, while the lower panel of each column corresponds to off-contact of the beam to the tissue with skin. Each of the two surface application methods were tested with the beam directing at three different regions of the spinal canal: (A) at site 1, (B) at site 5, and (C) at site 9. Irradiance peak values for off-contact illumination of the tissue without skin as depicted by the upper panel of (A) to (C) are as the following. A surface power of 4 W (1.27 W/cm^2) resulted in the peak irradiance of the device specific saturation level of > 41 μW/cm^2 when directing at sites 1 and 5. When the beam was directed to site 9, a surface power of 10 W (3.14 W/cm^2) resulted in a maximum of 13.1 μW/cm^2 measured at PD sensors 7 and 8. Irradiance peak values for off-contact illumination of the tissue with skin as depicted by the lower panel of (A) to (C) are as the following. When the beam was directed respectively to site 1, site 5, and site 9, a surface power of 10 W (3.14 W/cm^2) resulted in a maximum irradiance of respectively 2.9 μW/cm^2, 4.1 μW/cm^2, and 1.2 μW/cm^2 occurring at respectively the cranial, middle, and caudal aspects of the probe.

Figure 2 presents the intra-spinal irradiances over an 8-cm length of the spinal canal of dog 5 (34.35 kg) as measured by the nine-channel photodetector probe that differed in probe-skin contact. The upper panel of each column corresponds to off-contact of the beam to the tissue with skin, while the lower panel of each column corresponds to on-contact of the beam to the tissue with skin. Each of the two surface application methods were tested with the beam directing at 3 different regions of the spinal canal: (A) at site 1, (B) at site 5, and (C) at site 9. It is noted that the upper panel of Fig. 2 is the duplication of the lower panel of Fig. 1. Irradiance peak values for off-contact illumination of the tissue with skin as depicted by the upper panel of (A) to (C) are as the following: When the beam was directed respectively to site 1, site 5, and site 9, a

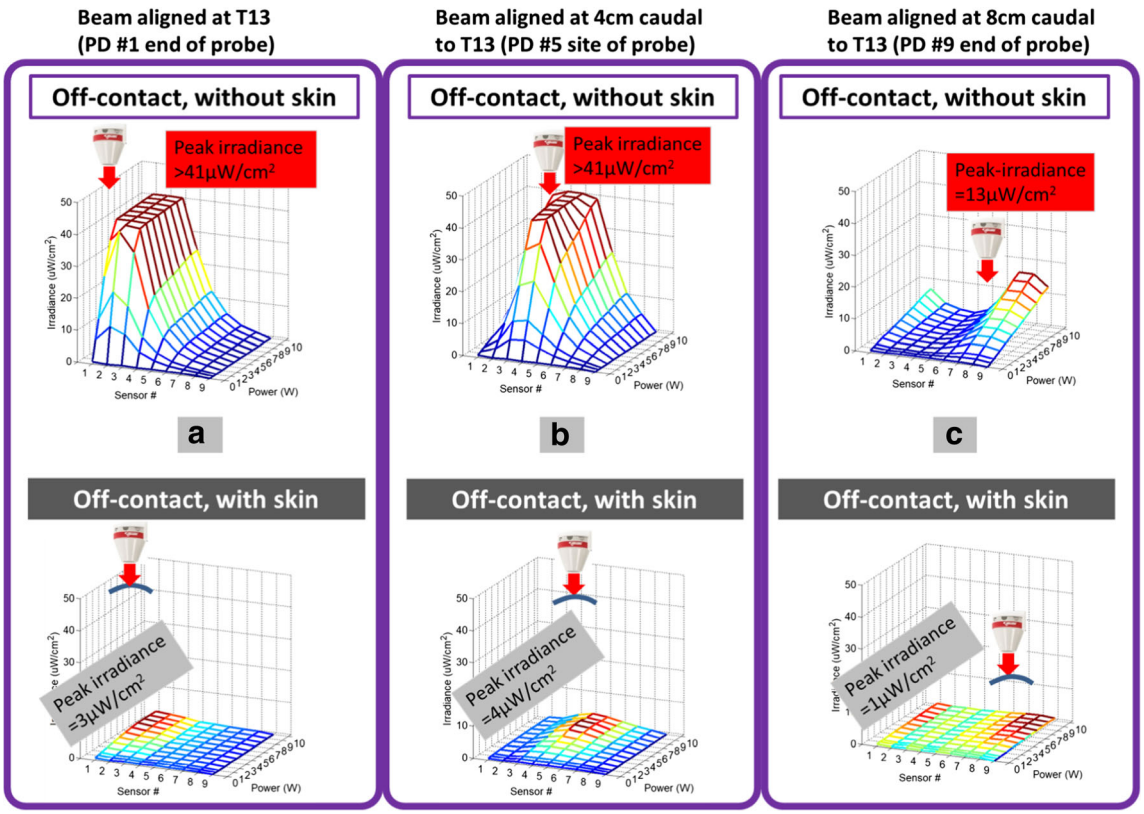

Fig. 1 Representative results of the intra-spinal irradiance distribution measured along an 8-cm column length by the nine-channel flexible photodetector probe. The upper panel and the lower panel of each column differ in skin transmission. **a** Beam directed to T13. **b** Beam directed to a spinal column site 4 cm caudal to T13. **c** Beam directed to a spinal column site 8 cm caudal to T13. The photodetector saturates at 41 μW/cm^2

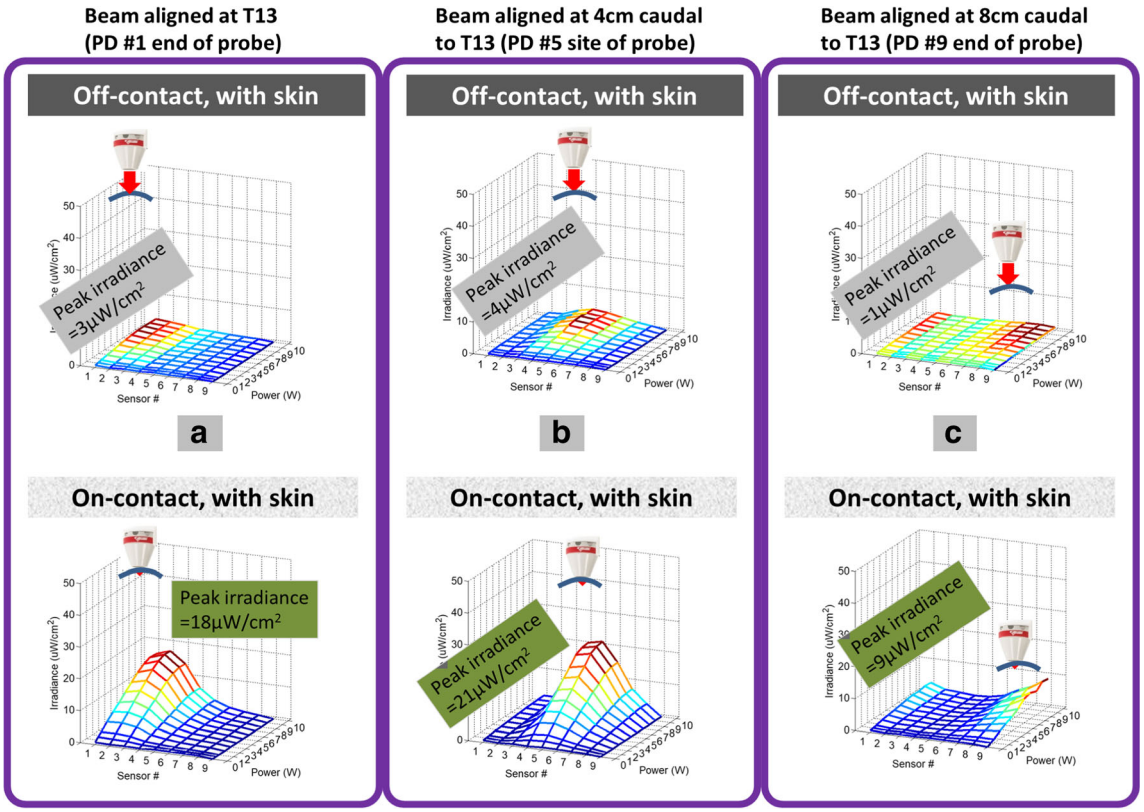

Fig. 2 Representative results of the intra-spinal irradiance distribution measured along an 8-cm column length by the nine-channel flexible photodetector probe. The upper panel and the lower panel of each column differ in probe-skin contact. **a** Beam directed to T13. **b** Beam directed to a spinal column site 4 cm caudal to T13. **c** Beam directed to a spinal column site 8 cm caudal to T13

surface power of 10 W (3.14 W/cm^2) resulted in a maximum irradiance of respectively 2.9 μW/cm^2, 4.1 μW/cm^2, and 1.2 μW/cm^2 occurring at respectively the cranial, middle, and caudal aspect of the probe. Irradiance peak values for on-contact illumination of the tissue covered by skin as depicted by the lower panel of (A) to (C) are as the following. When the beam was directed respectively to site 1, site 5, and site 9, a surface power of 10 W (3.14 W/cm^2) resulted in a maximum irradiance of respectively 17.6 μW/cm^2, 21.4 μW/cm^2, and 9.2 μW/cm^2 occurring at respectively the cranial, middle, and caudal aspect of the probe.

Intra-spinal irradiance as affected by the skin transmission

The effect of skin on transcutaneously applied 980 nm light is appreciated in Fig. 3. The intra-spinal irradiances at the nine PD sensors of the intra-spinal probe were measured with the surface illuminations applied off-contact from the tissue but differed in the skin transmission (without or with the skin). The means and SDs were averaged for four or six dogs as noted. The irradiance values are shown for a surface irradiance of 3.14 W/cm^2 or a corresponding surface power of 10 W. When saturation of the photodiode occurred at a surface irradiance lower than 3.14 W/cm^2, the local irradiance measured at a surface illumination power one step lower than the value causing saturation was scaled to project the value expected at a surface illumination of 3.14 W/cm^2.

Directing the beam to the surface site 1 as shown in (A) resulted in a peak irradiance of 234.0 ± 120.7 μW/cm^2 without the skin and 35.7 ± 33.3 μW/cm^2 with the skin, both measured at the cranial aspect of the intra-spinal probe. Comparing the mean and SD values with the skin and without the skin at all nine intra-spinal sites in four dogs (dogs 1 and 2 were not tested for this procedure) produced $p = 0.0203$, indicating that skin attenuated the surface applied 980 nm when administered at the surface site 1. The peak intra-spinal irradiance with the presence of skin was approximately 15% of that in the absence of skin. Directing the beam to the surface site 5 as shown in (B) resulted in a peak irradiance of 230.7 ± 178.3 μW/cm^2 without the skin and 50.9 ± 75.3 μW/cm^2 with the skin, both measured at the mid-region of the intra-spinal probe. Comparing the mean and SD values at all nine intra-spinal sites in six dogs produced $p = 0.0014$, indicating that skin attenuated the surface applied 980 nm when administered at the surface site 5. The peak intra-spinal irradiance with the skin was approximately 22% of that without the skin. Directing the beam to the surface site 9 as shown in (C) resulted in a peak irradiance of 130.2 ± 169.6 μW/cm^2 without the skin and 15.7 ± 16.3 μW/cm^2 with the skin, both measured at the caudal aspect of the intra-spinal probe. Comparing the mean

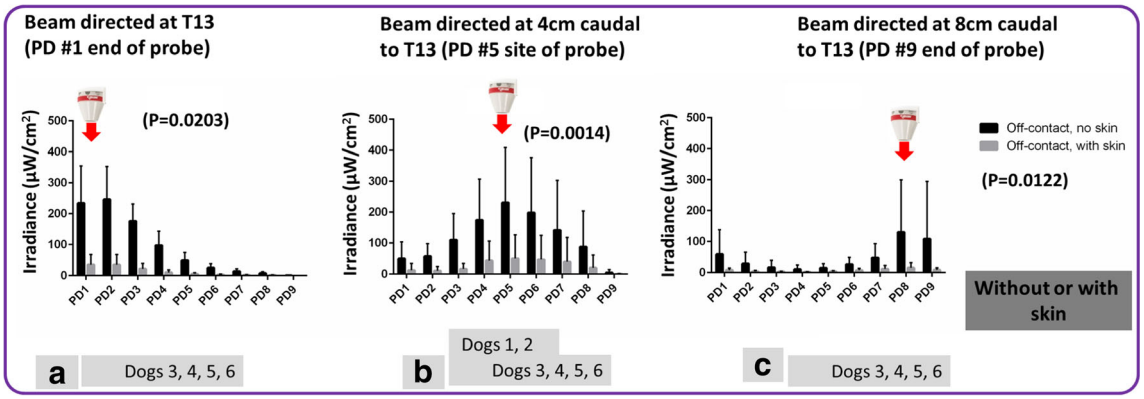

Fig. 3 Comparison of the irradiances at nine sites within the spinal canal for off-contact illuminations that differ in skin transmission. **a** Beam directed to T13 (aligned to PD sensor 1). $n = 4$. **b** Beam directed to a spinal column surface site 4 cm caudal to T13. $n = 6$. **c** Beam directed to a spinal column surface site 8 cm caudal to T13. $n = 4$

and SD values at all nine intra-spinal sites in four dogs (dogs 1 and 2 were not tested for this procedure) produced $p = 0.0122$, inferring that the skin attenuated the surface applied 980 nm when administered at the surface site 9. The peak intra-spinal irradiance in the presence of skin was approximately 12% of that in the absence of skin.

Intra-spinal irradiance as affected by the probe-skin contact

The effect of probe-skin contact on transcutaneously applied 980 nm light can be assessed in Fig. 4. The intra-spinal irradiances at the nine PD sensors of the intra-spinal probe were compared with the surface irradiance applied to the skin but differed in the probe-skin contact (off or on contact with the skin-covered tissue). The means and SDs were averaged for four or six dogs, as noted. The irradiance values are for a surface irradiance of 3.14 W/cm^2 or correspondingly a surface power of 10 W. When saturation of the photodiode occurred at the surface irradiance lower than 3.14 W/cm^2, the local irradiance measured at a surface irradiance power one step lower than the value causing saturation was scaled to project the value expected at a surface irradiance of 3.14 W/cm^2. The values that correspond to off-contact application with skin are the same as the set shown in Fig. 3.

Directing the beam to respectively the surface site 1, site 5, and site 9 as shown in (A), (B), and (C) resulted in a peak irradiance of 35.7 ± 33.3 μW/cm^2, 50.9 ± 75.3 μW/cm^2, and 15.7 ± 16.3 μW/cm^2 for the probe off-contact with skin and 44.6 ± 43.1 μW/cm^2, 85.4 ± 139.1 μW/cm^2, and 22.0 ± 23.6 μW/cm^2 for the probe on-contact with skin. The difference corresponded to $p = 0.0461$ for the beam directed to the surface site 1, $p = 0.0164$ for the beam directed to the surface site 5, and $p = 0.0216$ for the beam directed to the surface site 9, indicating that the on-contact application of the probe with skin at all three spinal locations enhances transcutaneous transmission. The peak intra-spinal irradiance by on-contact application was at a maximum of 67% higher than that of the off-contact application. The results from Figs. 3 and 4 are also summarized in Table 1.

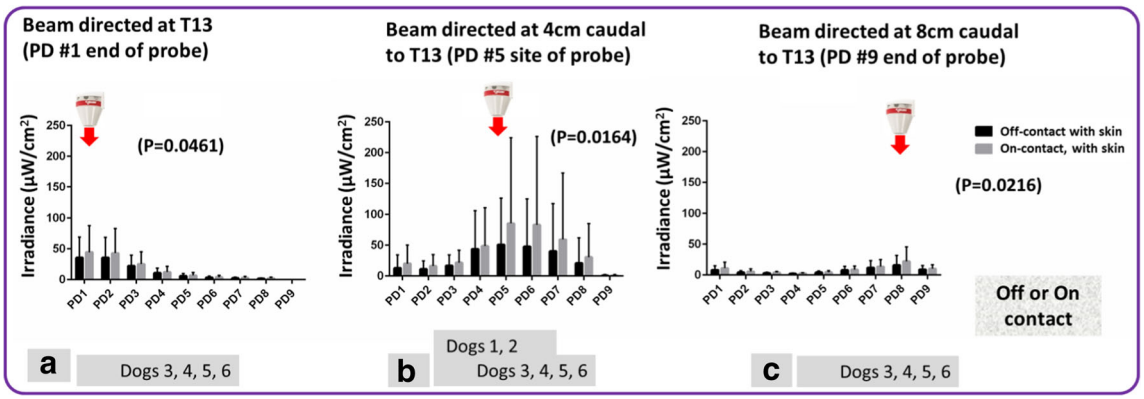

Fig. 4 Comparison of the irradiances at nine sites within the spinal canal with tissue covered by skin but differ in probe-skin contact. **a** Beam directed to T13. $n = 4$. **b** Beam directed to a spinal column surface site 4 cm caudal to T13. $n = 6$. **c** Beam directed to a spinal column surface site 8 cm caudal to T13. $n = 4$

Table 1 Peak intra-spinal irradiance among nine sites spaced approximately 1 cm apart, when under a surface irradiation of 10 W that corresponded to an irradiation of 3.14 W/cm^2. Any two cells marked with the same number of "*" represent that the same set of data is used in the two respective cells

	Beam at T13		Beam at 4 cm caudal to T13		Beam at 8 cm caudal to T13	
	OFF, NS	OFF, WS	OFF, NS	OFF, WS	OFF, NS	OFF, WS
(A) Illuminations applied at three positions but differed in skin transmission						
MN ± SD (μW/cm^2)	234.0 ± 120.7 (4 dogs)	*	230.7 ± 178.3 (4 dogs)	**	130.2 ± 169.6 (4 dogs)	***
		35.7 ± 33.3 (6 dogs)		50.9 ± 75.3 (6 dogs)		15.7 ± 16.3 (6 dogs)
	OFF, WS	ON, WS	OFF, WS	ON, WS	OFF, WS	ON, WS
(B) Illuminations applied at three positions but differed in probe-skin contact						
MN ± SD (μW/cm^2)	*		**		***	
	35.7 ± 33.3 (6 dogs)		50.9 ± 75.3 (6 dogs)		15.7 ± 16.3 (6 dogs)	
		44.6 ± 43.1 (4 dogs)		85.4 ± 139.1 (4 dogs)		22.0 ± 23.6 (4 dogs)

The measurements were averaged for four dogs or six dogs upon the availability of the data

OFF off-contact, *NS* no skin, *WS* with skin, *ON* on-contact

Discussion

The use of PBM for clinical applications is growing in its popularity as a non-invasive modality for a number of neurological diseases. Transcranial PBM at 610 nm and 800–810 nm is reported to improve cerebral neurological functions [9, 10] by means of near-infrared photons interacting with one or more light-sensitive chromophores including cytochrome C oxidase to boost cellular adenosine triphosphate (ATP) and reactive oxygen species (ROS) [9, 10]. Manifestations of cellular modulations by PBM in other clinical regimens vary [4, 5, 11, 15, 19], but the observations had included reducing inflammatory symptoms such as swelling and edema by using low-level non-thermal light at 660 nm, 780 nm, 808 nm, or 820 nm wavelengths [4, 5, 15, 19, 20]. In addition, indication for neuropathic benefit with the use of 980 nm transcutaneous irradiation has been noted [22]. The neuropathic changes that were induced by PBM at 980 nm included regeneration of the intra-epidermal nerve fibers, re-innervation of the Langerhan cells, and a decrease in expression of protein gen product 9.5 [22]. In vitro exposure of neuronal cells to 980 nm laser has been shown to modulate sodium channel proteins by laser-induced photothermal effect [23] and to improve neurite elongation (primary rat cortical neurons) by non-thermal means [24]. As the clinical goals of spinal cord intervention are to "rescue, reactivate, and rewire" the neuronal network, the impact on inflammation and nerve regeneration by PBM has exciting possibilities for neurologic injury and disease [3].

The benefit of PBM on the spinal cord in the clinical setting, particularly at 980 nm, remains speculative due to the inconsistent success in experimental models. In evaluating the application of 980 nm wavelength for neurologic injury or disease, the literature is equivocal. The use of longer near infrared wavelengths, including 980 nm [25], for neurological applications, has been discouraged in favor of shorter wavelengths, including 665 nm and 810 nm [26]. In the rat model, though, indications for neuropathic benefit with the use of 980 nm transcutaneous irradiation have been noted [22]. It has also been speculated that due to the relatively higher absorption by water in tissue, the therapeutic benefits of 980 nm PBM might be secondary to a photothermal impact rather than a photobiomodulative stimulation of cytochrome C oxidase in the mitochondrial respiratory chain [27]. As the mechanism by which 980 nm induces cellular responses is still unknown, understanding the achievable spinal cord level irradiances transmitted transcutaneously in large mammals facilitates improved clinical decision making and control of the surface irradiances for safer and more effective spinal cord intervention. The clinical application, if it will be practiced at 980 nm, will need to address the potential interplay of therapeutic thermal effect with the desired photobiomodulatory response at the spinal cord tissue level. For either thermal effect or photobiomodulatory response, the discovery of the mechanisms must contain the accurately estimated or experimentally rendered data of terminal irradiance of a specific wavelength of light delivered to the spinal cord level as a result of skin-to-spine transmission.

The physiological changes generated from PBM of cranial nervous tissue located below the skull cap is a motivation to pursue its use for the spinal cord nervous tissue, as theoretically it should have a similar impact on the tissue. Unfortunately, the anatomic differences between the cranium and the spinal cord are notable. Therefore, the clinical concern is whether the attenuation of light transmission through a more robust level of tissue and bone cover allows for a therapeutic target dose at the level of the

spinal cord. In order to determine the effects of PBM on the spinal cord and surrounding tissues, it is essential to understand the dosimetry of PBM as it is transmitted through skin and underlying tissue and bone to reach the target site.

Utilizing a flexible nine-channel photodetector probe, this work was able to quantitate the local light irradiances at the level of the spinal canal (T13-L5) under a surface illumination of 980 nm (CW, 10 W, 3.14 W/cm^2 surface irradiance) in six cadaver dogs. The maximum irradiance measured at the inner surface of the spinal canal of the cadaver dogs was 0.231 ± 0.121 mW/cm^2 (off-contact, no skin) and 0.051 ± 0.075 mW/cm^2 (in-contact, no skin). As 3.2 mW/cm^2 is the currently known target-level irradiance for spinal cord therapeutic response, this energy application does not appear to meet that threshold. The energy dose measured at the level of the spinal canal, when the beam was directed off-contact, with no skin, was 0.234 ± 0.121 mW/cm^2 (T13), 0.231 ± 0.178 mW/cm^2 (4 cm caudal to T13), and 0.130 ± 0.170 mW/cm^2 (8 cm caudal to T13). When the beam was directed off-contact, with non-haired skin, the irradiances measured were 0.036 ± 0.033 mW/cm^2 (T13), 0.051 ± 0.075 mW/cm^2 (4 cm caudal to T13) and 0.016 ± 0.016 mW/cm^2 (8 cm caudal to T13). This corresponds to a skin transmission of 15% at the level of T13, 22% at 4 cm caudal to T13, and 12% at 8 cm caudal to T13. In comparison to off-contact application, the energy dose measured at the level of the spinal canal when the beam was placed on-contact with non-haired skin and was 0.045 ± 0.043 mW/cm^2 (T13), 0.085 ± 0.139.1 mW/cm^2 (4 cm caudal to T13), and 0.022 ± 0.024 mW/cm^2 (8 cm caudal to T13). On-contact application significantly increased the target dosage by 25% at T13, 67% at 4 cm caudal to T13, and 40% at 8 cm caudal to T13. This finding implores the use of direct surface contact to increase target dosage.

Due to the novel nature of this undertaking, the authors recognize the limitations of this research model. In order to accommodate the diameter of the inter-spinal probe, a large hemi-laminectomy site was needed. This surgical approach removed a significant amount of bone on the lateral aspect of the spinal canal. Although the laser headpiece was placed on the opposing side of the spinal canal and the open area was filled with tissue, this incomplete vertebral closure may account for a difference in target-level irradiance. In addition, this type of research with large hemi-laminectomy cannot be accomplished with living tissue; therefore, the use of cadaverous tissue has caused the following limitations that must be considered for clinical applications. There are also differences in the optical properties between normal and cadaverous tissues which could influence the target-level irradiance distribution and light transmission [28, 29]. The lack of hydration and blood flow diminishes the ability to make allowances for the absorption of light by water, oxygenated hemoglobin and deoxygenated hemoglobin in the heavily muscled tissue surrounding the spinal canal in the cadaverous tissue [30]. Cadaverous tissue certainly becomes compromised with handling (freeze, thaw) and may have light transmission properties that differ from living tissue [31]. The cadavers utilized were all dark-skinned male dogs with variable skin, soft tissue and bone thicknesses (height, width). Although the use of varying skin colors is attractive, the use of all dark-skinned dogs helped to reduce confounding factors by removing an important variable. The difference in tissue thicknesses is a reflection of anatomical diversity that is a clinical consideration in any population. In the future, the authors will work to include female dogs to highlight any differences between the sexes.

Future studies should also focus on efforts to provide a clinically therapeutic PBM dose to the spinal cord by overcoming the anatomic safeguards preventing light transmission. Replicating this study to evaluate differing wavelengths with neurologic PBM potential would be beneficial to determine the most proficient wavelength for skin-to-spine penetration. This undertaking will require benchmarking the spectral responsivities of the photodetector sensor array at the individual wavelengths. In addition, it would be necessary to produce treatment lasers which emit the same output power at the multiple wavelengths and provide a light delivery configuration that can remain fixed over the tissue surface for skin-to-spine transmission while allowing switching among the multiple laser wavelengths. As this study highlighted, the skin significantly attenuates PBM light transmission. Therefore, future work needs to be done to evaluate means to overcome the skin barrier. The prospect of assessing the use of contact mediums which render the skin transparent to PBM light is exciting. This novel skin clearing technique may enhance the opportunity for the most clinically appropriate PBM wavelength to overcome the skin barrier, increasing the probability of reaching the target therapeutic irradiance of 3.2 mW/cm^2 at the level of the spinal cord. Furthermore, this technique may also eliminate the concern for collateral damage to surface tissues.

Collectively, the intra-spinal deployment of the flexible probe that required the use of cadaveric tissue was the most a significant limitation to this study. In order to overcome this limitation, future investigations require the development of a petite version of the flexible probe. Probe size reduction will allow for a less invasive surgical approach to the spinal canal, which will pave the way for irradiance to be measured in real time in a live animal.

Although limitations existed, this is the first reported dosimetry of transcutaneous transmission of 980 nm light to the spinal canal of large companion animals of clinically relevant sizes in both number and weight. The maximal irradiances measured at the inner surface of the spinal canal of the cadaver dogs under a surface irradiance of 3.14 W/cm^2 were 0.231 ± 0.121 mW/cm^2 when the light was directed off-contact without skin and 0.051 ± 0.075 mW/cm^2 when the beam was applied by the treatment head on-contact with the skin.

Conclusions

PBM is a non-invasive intervention that has the opportunity to reduce inflammation, confer analgesia, and stimulate healing of neuronal tissue. Unfortunately, the anatomic safeguards, such as heavy muscle cover and thick skeletal bone, protecting the central nervous system are the most difficult for light to overcome. In order to determine if any wavelength of light has an impact on the spinal cord, it is essential to define the treatment parameters necessary to safely obtain the target level irradiance needed to produce a therapeutic response. Our team's objectives were to report the target level irradiance at the level of the spinal canal using transcutaneous transmission of 980 nm light in six large breed cadaver dogs and evaluate surface application technique's effect on target-level dosage: the use of 980 nm, 10 W, or 3.14 W/cm^2, CW illumination on-contact transmitted to the spinal canal 44.6 ± 43.1 μW/cm^2 at T13, 85.4 ± 139.1 μW/cm^2 at 4 cm caudal to T13, and 22.0 ± 23.6 μW/cm^2 at 8 cm caudal to T13. This irradiance falls below the 3.2 mW/cm^2 target-level irradiance reported to produce a therapeutic response. In addition, this data confirms that the skin is a significant impediment to PBM transmission; on-contact application of the PBM treatment probe should be utilized in the clinical environment to increase PBM dose transmission.

Future investigations should be focused on overcoming the skin barrier, as well as muscle and bone anatomic safeguards for testing in the live animal. To accomplish this task, different PBM wavelengths must be evaluated to determine if delivering therapeutic irradiance to the spinal cord is possible. The use of a skin clearing contact medium with an on-contact PBM probe may also potentially eliminate the skin as a barrier to PBM dose transmission, reducing attenuation to effectively increasing skin-to-spine PBM dose transmission. The development of a petite version of the flexible probe is under consideration to offer the opportunity for a less invasive surgical approach to the spinal canal, allowing for target irradiance to be measured in the live animal. These prospective investigations have the opportunity to provide for clinically relevant recommendations on PBM spinal cord interventions.

Funding information LiteCure LLC.

Compliance with ethical standards

Conflict of interest L. DeTaboada has financial interest in LiteCure LLC which produced the laser unit used for this study. D. Piao received a grant from LiteCure LLC for directing this work. No other conflicts of interest exist for this study.

Ethical approval The use of cadaver dogs for this study was exempted by the Institutional Animal Care and Use Committee of Oklahoma State University.

References

1. Byrnes KR et al (2005) Light promotes regeneration and functional recovery and alters the immune response after spinal cord injury. Lasers Surg Med 36(3):171–185
2. de Andrade ALM, Bossini PS, Parizotto NA (2016) Use of low level laser therapy to control neuropathic pain: a systematic review. J Photochem Photobiol B Biol 164:36–42
3. Ramer LM, Ramer MS, Bradbury EJ (2014) Restoring function after spinal cord injury: towards clinical translation of experimental strategies. Lancet Neurol 13(12):1241–1256
4. Meireles A et al (2012) Avaliação do papel de opioides endógenos na analgesia do laser de baixa potência, 820 nm, em joelhos de ratos Wistar. Rev Dor 13(2):152–155
5. Serra AP, Ashmawi HA (2010) Influência da naloxona e metisergida sobre o efeito analgésico do laser em baixa intensidade em modelo experimental de dor. Rev Bras Anestesiol 60(3):302–310
6. Hawkins D, Abrahamse H (2007) Phototherapy—a treatment modality for wound healing and pain relief. Afr J Biomed Res. 10(2);99–109. http://www.bioline.org.br/pdf?md07014
7. Ando T et al (2013) Low-level laser therapy for spinal cord injury in rats: effects of polarization. J Biomed Opt 18(9):098002
8. Wu X et al (2009) 810 nm Wavelength light: an effective therapy for transected or contused rat spinal cord. Lasers Surg Med 41(1): 36–41
9. Salehpour F et al (2017) Transcranial low-level laser therapy improves brain mitochondrial function and cognitive impairment in D-galactose-induced aging mice. Neurobiol Aging 58:140–150
10. Salehpour F et al (2018) Transcranial near-infrared photobiomodulation attenuates memory impairment and hippocampal oxidative stress in sleep-deprived mice. Brain Res 1682: 36–43
11. Karlekar A et al (2015) Assessment of feasibility and efficacy of class IV laser therapy for postoperative pain relief in off-pump coronary artery bypass surgery patients: a pilot study. Ann Card Anaesth 18(3):317
12. Brock JA, McAllen RM (2016) Spinal cord thermosensitivity: an afferent phenomenon? Temperature 3(2):232–239
13. Janzadeh A et al (2017) Combine effect of chondroitinase ABC and low level laser (660 nm) on spinal cord injury model in adult male rats. Neuropeptides 65:90–99
14. Hu D, Zhu S, Potas JR (2016) Red LED photobiomodulation reduces pain hypersensitivity and improves sensorimotor function following mild T10 hemicontusion spinal cord injury. J Neuroinflammation 13(1):200
15. Rochkind S et al (2002) Transplantation of embryonal spinal cord nerve cells cultured on biodegradable microcarriers followed by low power laser irradiation for the treatment of traumatic paraplegia in rats. Neurol Res 24(4):355–360
16. Paula AA et al (2014) Low-intensity laser therapy effect on the recovery of traumatic spinal cord injury. Lasers Med Sci 29(6): 1849–1859
17. Veronez S et al (2017) Effects of different fluences of low-level laser therapy in an experimental model of spinal cord injury in rats. Lasers Med Sci 32(2):343–349
18. Sotoudeh A et al (2015) The influence of low-level laser irradiation on spinal cord injuries following ischemia-reperfusion in rats. Acta Cir Bras 30(9):611–616
19. da Silva T et al (2018) Effect of photobiomodulation treatment in the sublingual, radial artery region, and along the spinal column in

individuals with multiple sclerosis: protocol for a randomized, controlled, double-blind, clinical trial. Medicine 97(19):e0627
20. da Silva FC et al (2018) Photobiomodulation improves motor response in patients with spinal cord injury submitted to electromyographic evaluation: randomized clinical trial. Lasers Med Sci 33(4): 883–890
21. Piao D et al (2018) Flexible nine-channel photodetector probe facilitated intraspinal multisite transcutaneous photobiomodulation therapy dosimetry in cadaver dogs. J Biomed Opt 23(1):010503
22. Saidu E et al (2013) 980 nm Wavelength light decreases mechanical allodynia in a rat neuropathic pain model. Lasers Surg Med 45:51–51
23. Li X et al (2014) 980-nm infrared laser modulation of sodium channel kinetics in a neuron cell linearly mediated by photothermal effect. J Biomed Opt 19(10):105002
24. Anders JJ et al (2014) In vitro and in vivo optimization of infrared laser treatment for injured peripheral nerves. Lasers Surg Med 46(1):34–45
25. Hashmi JT et al (2010) Role of low-level laser therapy in neurorehabilitation. PM R 2(12 Suppl 2):S292–S305
26. Wu Q et al (2012) Low-level laser therapy for closed-head traumatic brain injury in mice: effect of different wavelengths. Lasers Surg Med 44(3):218–226
27. Hamblin MR (2018) Mechanisms and mitochondrial redox signaling in photobiomodulation. Photochem Photobiol 94(2):199–212
28. Pitzschke A et al (2015) Optical properties of rabbit brain in the red and near-infrared: changes observed under in vivo, postmortem, frozen, and formalin-fixated conditions. J Biomed Opt 20(2):25006
29. Sterzik V et al (2014) Spectrometric evaluation of post-mortem optical skin changes. Int J Legal Med 128(2):361–367
30. Wilson BC, Jeeves WP, Lowe DM (1985) In vivo and post mortem measurements of the attenuation spectra of light in mammalian tissues. Photochem Photobiol 42(2):153–162
31. McElderry JD, Kole MR, Morris MD (2011) Repeated freeze-thawing of bone tissue affects Raman bone quality measurements. J Biomed Opt 16(7):071407